Hyperfine Interact (2015) 236:9–18
DOI 10.1007/s10751-015-1189-x

Preparation of cold ions in strong magnetic field and its application to gas-phase NMR spectroscopy

K. Fuke[1,2] · Y. Ohshima[3] · M. Tona[4]

Published online: 14 May 2015

Abstract Nuclear Magnetic Resonance (NMR) technique is widely used as a powerful tool to study the physical and chemical properties of materials. However, this technique is limited to the materials in condensed phases. To extend this technique to the gas-phase molecular ions, we are developing a gas-phase NMR apparatus. In this note, we describe the basic principle of the NMR detection for molecular ions in the gas phase based on a Stern-Gerlach type experiment in a Penning trap and outline the apparatus under development. We also present the experimental procedures and the results on the formation and the manipulation of cold ions under a strong magnetic field, which are the key techniques to detect the NMR by the present method.

Keywords Nuclear magnetic resonance · Gas-phase molecular ions · Ultracold ion

1 Introduction

Nuclear magnetic resonance (NMR) technique is widely used for the physical and chemical analysis of various materials in liquid and solid phases [1]. Although this technique has been

Proceedings of the 6th International Conference on Trapped Charged Particles and Fundamental Physics (TCP 2014), Takamatsu, Japan, 1-5 December 2014

✉ K. Fuke
fuke@kobe-u.ac.jp

[1] Institute for Molecular Science, Myodaiji, Okazaki, Japan

[2] Graduate School of Science, Kobe University, Rokkodai, Nada-ku, Kobe, Japan

[3] Department of Chemistry, Tokyo Institute of Technology, O-okayama, Meguro-ku, Tokyo, Japan

[4] Ayabo Co. Fukukama, Anjo, Japan

well established, it requires a large amount of samples and also, sometimes, the purification and crystallization limit the structural analysis. In order to compensate these problems, recently, mass spectroscopic techniques are widely used in various research fields [2]. Since this method gives information only on the mass number, many research groups use it to reconstruct the structures of the parent molecular ions with an aid of the computer simulations for the fragment ions [3]. Especially, if the target molecular ion includes an isomer, which has the same mass number and the different geometrical structure, the assignment of geometrical structure becomes much difficult. Under these circumstances, a new extension of the NMR technique to the gas-phase molecular ions, which enables us to obtain rich information on the structure of the target ions with a mass-spectral sensitivity, becomes increasingly important in both fundamental and applied sciences. Historically, the NMR spectroscopy was first used for studying the magnetic moment of isolated atoms and molecules by Rabi and coworkers [4]. They succeeded in determining the magnetic moments by developing a molecular beam magnetic resonance technique based on the Stern-Gerlach experiment. Unfortunately, this technique utilized to neutral species is not applicable to the gas-phase ions, because the ions cannot be confined under the strong wedge-type magnetic field. Quite recently, Ulmer and his coworkers successfully reported a first NMR detection of a single trapped proton [5] with a continuous Stern-Gerlach experiment similar to that developed by Dehmelt [6]. However, this technique is limited to light nuclei, because they need a much stronger inhomogeneous field to detect a spin flip of the heavier nuclei.

In order to resolve the aforementioned problems on the structural analysis of the gas-phase molecular ions, we proposed a new method, called "magnetic resonance acceleration" technique, in our previous paper [7]. The outline of our detection method will be described in Experimental Section. Briefly, we adopt a long Penning-type trap as a NMR cell and place it in a bore of superconducting magnet, which has two homogeneous field regions with high and low magnetic fields and a strong gradient field in between [8]. To detect a weak NMR signal, two radio frequency (RF) coils are installed next to the trapping electrodes in the NMR cell to flip the nuclear spin of the ions synchronized with the shuttle motions of the ions. This configuration allows multiple interaction between the magnetic moment of the ions with the gradient magnetic field and realizes a continuous Stern-Gerlach experiment for the trapped ions.

As in the Rabi's method, the key techniques of the present method to detect the NMR signal lie in the formation of cold molecular ions and their manipulation. Until now, various methods have been developed for cooling neutral atoms and molecules [9]. For atomic and diatomic ions, a variety of sophisticated techniques have been developed, such as the laser based cooling methods [10]. A sympathetic cooling is an interesting technique to cool complex molecular ions [11, 12]. However, it is difficult to combine these techniques to the device for the NMR detection, which requires an extremely homogeneous magnetic field region for conducting a high-resolution magnetic resonance experiment. Although ions are easy to manipulate with electric and magnetic fields, slow ions are very sensitive to stray fields and space charge. Especially, when the trapping space is large as in the case of our apparatus, it becomes very difficult to prepare cold molecular ions and manipulate them [10].

In the present study, we newly design and construct the ion source and the NMR cell containing the RF coils to reduce the effect of stray fields. As mentioned above, the present method requires the ultracold ion packets with a slow velocity and an extremely narrow velocity distribution width. In order to develop the cooling technique of molecular ions, we explore the methods to decelerate the ion packets and bunch them under the strong magnetic

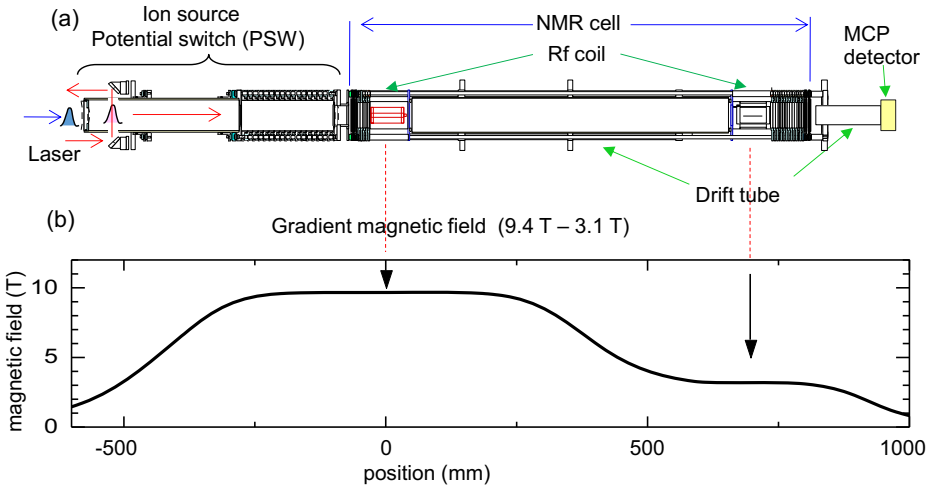

Fig. 1 **a** Experimental setup for the potential switch and the NMR cell. A small hole on the drift tube of potential switch is a window for introducing the photoionization laser. **b** Magnetic field distribution of the superconductive magnet. The scales of these figures are the same and, the arrows indicate the center of the high and low homogeneous magnetic field regions

field by using a potential switch and a velocity selection. Here, we outline the principle of the gas-phase NMR detection. We further describe the features of the newly developed apparatus and discuss on the experimental results on the preparation and manipulation of cold molecular ions.

2 Experimental method

2.1 Principle of NMR detection

A detailed description of our method was published previously [7] and so only the essential details of the experiment scheme are summarized below. The present method is a new extension of the Rabi's technique for neutral molecules. In their technique, they detected a deviation of the radial distribution of molecular beam [4], which is induced by the interaction of nuclear magnetic moment with a strongly gradient magnetic field generated by a wage-type magnet aligned in the beam direction. Because the molecular ion beams cannot be confined under the gradient magnetic field, we newly design a Penning trap for the NMR cell to conduct the Stern-Gerlach type experiment. Figure 1a shows a scheme of our experimental setup, which is installed in the bore of the superconducting magnet. The magnet has two homogeneous field regions with high ($B_{\mathrm{H}} = 9.4$ T) and low magnetic ($B_{\mathrm{L}} = 3.1$ T) fields as shown in Fig. 1b [7, 8], where a magnetic resonance excitation of the ions is performed with two different oscillatory fields. The above two regions are connected with a steep gradient field region, where the ions experience the magnetic force in the axial direction. The front and back gates are placed at near the 9.4 T and 3.1 T regions, respectively, to store the ions in the z direction. When the ions are injected into the cell, they are confined from escaping in thexy plane under the strong axial magnetic field by virtue of a cyclotron motion. As described in the previous paper [7], the features of the NMR cell allow us to

treat the motion of the ion packet as a pseudo one dimensional one along the magnetic field. Thus, with the present setup, the ions are forced to move back and forth along the magnetic field and the interaction time with the gradient field increases with increasing the number of round-trips. And also, the measurement of a time-of-flight (TOF) of the ions allows us to detect the effect of magnetic interaction on the axial velocity.

The scheme of our NMR detection is as follow. When the ions with a slow initial mean velocity (v_0) and a sufficiently narrow velocity distribution width (Δv_0) are introduced into the NMR cell through the front gate, they move along the z axis and are accelerated (and/or decelerated) at the gradient-field region by the force generated through the interaction of the magnetic field gradient ($\mathrm{d}B/\mathrm{d}z$) with both the nuclear magnetic moment (μ_N) and the magnetic moment (μ_C) induced by the cyclotron motion. Since a nuclear spin relaxation time of a gas-phase closed-shell ion is usually longer than 1 s, a velocity change induced by the magnetic interaction is cancelled out after each round-trip, that is, the ions experience the opposite force in the back and force motions. Thus, under a collision free condition, the trapped ions keep on moving back and forth for a long time. In order to get the NMR information, we install the pair of RF coils in the high and low homogeneous field regions as shown in Fig. 1a. By synchronously applying the weak RF magnetic fields with two resonance frequencies so called a π-pulse to the ions at each time when they pass through the coils, the nuclear spins flip if a resonance condition is fulfilled. With this scheme, the translational velocities of the ions in the different nuclear spin states increase or decrease continuously with increasing the number of round trips. After an appropriate number of round-trips (N), the ions with the different nuclear spin states are spatially separated in the z direction ("spin polarization"). This change can be observed by measuring the TOF profile of the ion packet released from the NMR cell with a microchannel plate (MCP) detector. As described in the previous paper [7], the measurements of the time profiles as a function of the RF frequency allow us to determine the nuclear magnetic moment and a Larmor frequency of the proton (ω) in the molecular ions. It should be noted that the frequencies of two coils installed at the high and low magnetic fields should satisfy a condition that $\omega_\mathrm{H}/\omega_\mathrm{L} = B_\mathrm{H}/B_\mathrm{L}$, where ω_H and ω_L are the Larmor frequencies of proton at two homogeneous fields; about 400.28 and 132.17 MHz for proton nuclei, respectively.

The present method enables us to detect the spatial spin polarization in the axial direction by narrowing the translational velocity distribution, that is, by cooling the translational temperature of the molecular beam. The detection sensitivity of the spin polarization is mainly determined by the initial conditions of the translational motions of the sample ions; mean velocity (v_0), velocity distribution width (Δv_0; full width half maximum), and temporal width (τ_0). Under the gradient magnetic field, the force ($\boldsymbol{F}$) acts on nuclear spin is given by $F_z = \mu_N dB(z)/dz$, where μ_N is the z component of the magnetic moment ($\mu_\mathrm{N} = \gamma\ (\mathrm{h}/2\pi)\ m_\mathrm{I}$); m_I is a nuclear spin quantum number (= 1/2). A simple calculation gives the velocity increase (Δv) as

$$\Delta v = (\mu_\mathrm{N}/M v_0)(B_\mathrm{H} - B_\mathrm{L})(2N + 1), \tag{1}$$

where M is the mass of the ion. μ_N is 1.41 x 10^{-26} J T^{-1} for proton. In the case of molecular ion having n_p protons with the same chemical environment (Larmor frequency), Δv for the nuclear spin state having the highest total quantum number is given by multiplying n_p to (1). An estimation of magnetic resonance acceleration was described in the previous paper [7]. Similar calculations for the NH_3^+ ions predict the number of round trips (N) as $N \geq 4$ to detect the spin polarization with the initial conditions as $v_0 = 100$ m/s (1.8 meV), $\Delta v_0 = 0.4$ m/s, and $\tau_0 = 50\ \mu$s. These estimations indicate that the present method requires

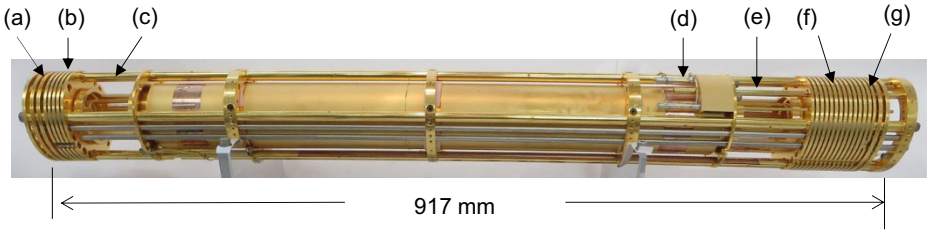

Fig. 2 Photograph of the NMR cell: (**a**, **g**) mesh electrode pairs, (**b**, **f**) cylindrical electrodes, (**c**, **e**) RF coils, (**d**) coil tuning unit consisting of non-magnetic trimer capacitors

the ions with very slow velocity with a narrow velocity width to observe the spatially well resolved spin polarization. Thus, as in the case of the Rabi's experiment, it is important to establish the technique to cool the translational temperature of the ions by narrowing the distribution width of the longitudinal velocity.

2.2 Experimental setup

In the present experiment, we adopt the photoionization of a supersonically cooled molecular beam to precool the ions. The ion source system consists of two differentially evacuated chambers separated by a 2-mm-diameter skimmer, which are evacuated by turbo molecular pumps. A pulsed valve (Jordan, PSV) is placed 20 mm upstream of the skimmer. The molecular beam is collimated further with another 5-mm-diameter skimmer installed at 800 mm downstream from the pulsed valve and is introduced into a third chamber, which is evacuated with a cryopump down to below 10^{-7} Pa. Figure 1 shows a schematic drawing of the experimental setup for the photoionization source working as a potential switch and the NMR cell. In the present study, both the ion source and the NMR cell are newly constructed to improve the cooling condition of the ions. The ion source, which consists of a 400 -mm length drift tube and cylindrical electrodes, is placed at the upstream of the NMR cell. The photoionization laser is crossed with the neutral beam through a hole located at the wall of the drift tube as shown in Fig. 1a. To facilitate the deceleration and the compression of the ion packet, the potential switch consisting of 17 cylindrical electrodes are divided into two parts. The first part is used as a buncher, while the second part is used to generate a potential slope for the deceleration. The drift tube and cylindrical electrodes are biased through a series chain of non-magnetic resistors.

The NMR cell shown in Figs. 1a and 2 is the Penning-type trap with an effective length of 744 mm. The front and back gates of the trap are made of five cylindrical electrodes and store the ion packet for a long time without a loss of the ions. On the other hand, the mesh electrode pairs installed both at the upstream of the front gate and at the downstream of the back gate work as a velocity selector for slicing the velocity distribution, as described in the next section. A pair of the home-made saddle-type RF coils are mounted just at the downstream and the upstream of the front and back gates, respectively. These coils are placed exactly at the center of the high (9.4 T) and low (3.1 T) homogeneous magnetic field regions as shown in Fig. 1 and are aligned parallel to the magnetic axis so as to generate the RF magnetic fields in the direction perpendicular to the ion beam. All electrodes and the RF coils are made of Au/Ag plated copper. The circuit including the RF coils is tuned by two closely-located non-magnetic capacitors (see (d) in Fig. 2); they are adjusted from the

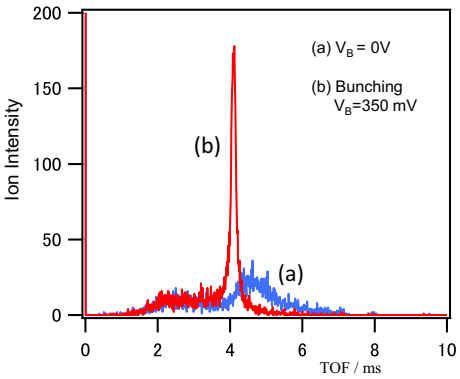

Fig. 3 Time-of-flight profiles of the NH_3^+ ions without (**a**) and with the bunching process (**b**). The bunching voltage is $V_B = 350$ mV

outside of the vacuum. The basic performance of these coils as the NMR probe is examined by measuring a proton NMR spectrum of a liquid-water sample tube placed in the coil.

As described in the next section, we have to prepare the ions with a very small kinetic energy. To manipulate the ions in the NMR cell, a baking process is indispensable; in fact, without the baking, the ions with the kinetic energy of less than 100 meV do not pass through the NMR cell. A possible cause of this defect is considered to be the mesh electrodes installed in the NMR cell, where the ions come closest to metal surfaces and may be influenced by a patch effect. In the present study, we also newly developed a non-magnetic baking system to heat the whole NMR cell up to 400 K.

3 Formation and manipulation of cold ion packet

In order to prepare the ions with a slow velocity of a very narrow velocity distribution width, the ions are cooled by three steps. We start with a supersonic molecular beam to precool the neutral molecules. The photoionization of the molecular beam enable us to form the cooled ion packet as cold as less than 10 K [13]. The molecular ions produced by these procedures are internally cold and have a narrow relative velocity distribution. However, the mean velocity of the ions in the laboratory frame is relatively high, and it depends on the temperature and the pressure of the source as well as the mass of the carrier gas employed [13]. The present experiment requires much lower mean velocity and velocity distribution width. Thus, in the second step, the ions produced are cooled by the bunching and deceleration using the potential switch. And then, the ions are transferred to the NMR cell and cooled further by a velocity selection procedure, in which the velocity distribution is reduced by cutting out a part of the ion packet with the mesh electrode pair. In the following sections, we describe the details of these experimental results for the formation and manipulation of the cold ion packet.

3.1 Deceleration and bunching of ion packet.

A mixture gas of NH_3 with Ar is expanded through the pulsed valve with a nozzle diameter of 0.5 mm. To facilitate the formation of monomer NH_3^+ ions, we use an amplified output of a picosecond laser pulse at 193 nm (20 ps, 3 mJ) as the photoionization light source by using an ArF excimer laser. A seed laser light at 193 nm is generated by mixing the fundamental of a picosecond YAG laser (EKSPLA PL2143) with the second harmonic of an optical parametric output at 236.6 nm. Figure 3 displays the TOF profile of the ions produced in

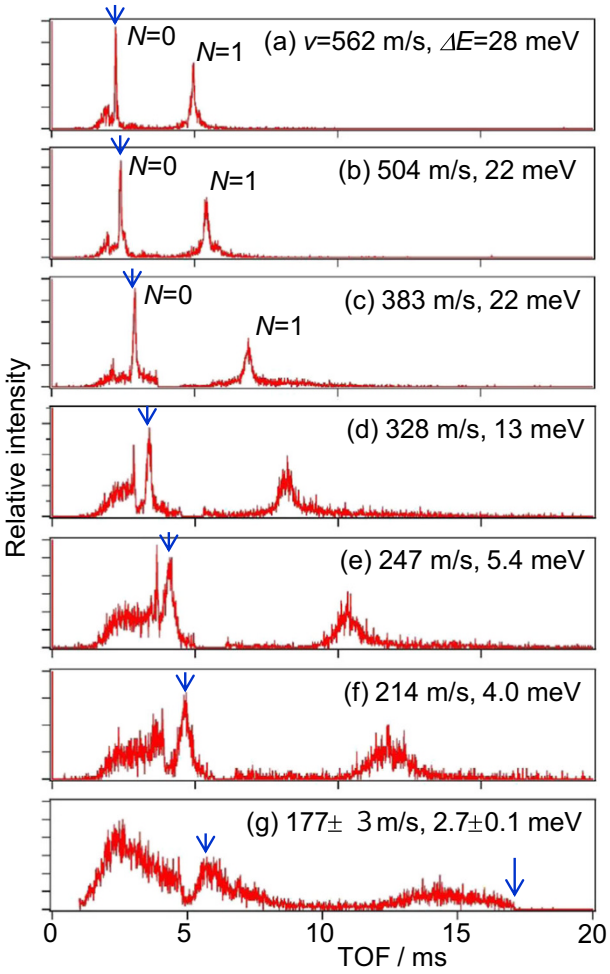

Fig. 4 Time-of-flight profiles of the NH_3^+ ions at various deceleration potentials. The mean velocities after the deceleration are indicated with the kinetic energy. The peaks with the arrows (noted as $N = 0$) are those directly reached to the MCP without reflection at the back gate, while those at the longer TOF (note as $N = 1$) correspond to the ion packets reached after one round-trip in the NMR cell. The second arrow at 17 ms in Fig. 4g indicates the transmission limit of the decelerated ions

the ion source. The curve (a) corresponds to the ion signals without the bunching. The ion signals consist of two broad peaks, in which the slower peak corresponds to the NH_3^+ ions. The weaker peak reached earlier to the detector is assigned to the aggregate ions such as $NH_4^+(NH_3)_n$. In the bunching process, the pulsed voltage is applied to the buncher with a suitable delay time after the photoionization laser. The curve (b) in Fig. 3 shows the result of the bunching with the pulsed voltage of 350 mV. By this procedure, the monomer ions are selectively bunched and their velocity distribution becomes very narrow without changing the mean velocity significantly.

These ions are decelerated by applying a continuous voltage to the rest of the cylindrical electrodes, which work as the potential switch. Figure 4a shows the TOF profiles for the NH_3^+ ions obtained by setting the voltage of the potential switch to 0 V. Here, the peak

denoted as N =0 corresponds to the time profile for the NH_3^+ ions directly reached to the MCP, while the weak peak appeared at a shorter TOF corresponds to those for the aggregate ions as mentioned previously. On the other hand, the peak denoted as N =1 corresponds to the NH_3^+ ions reached after a round-trip in the NMR cell. The latter profile is obtain by changing the potentials of the front and back gates from 0 to 0.3 V immediately after the ions pass through the front gate. And then, by decreasing the back-gate potential to 0 V after an elapsed time of a round-trip, the ion packet escapes from the cell and is detected by the MCP. The velocity of the ions in the NMR cell is determined by measuring the time difference between these two peaks as 562 m/s. We can also record the time profile of the ion packet for any desired number of round-trips by the similar procedures. In the figure, these two time profiles are superimposed. By increasing the degree of deceleration, the relative intensities of the aggregate ions increase in comparison with that of the monomer ions as seen in Fig. 4. These ions fly with the same velocity as the monomer ions and are detected at the same arrival time when they do not decelerate. However, the deceleration potential causes the velocity difference and separates these ions in the time of flight because the cluster ions are heavier than the monomer and possess a lager translational energy. Hereafter we concentrate on the analysis for the monomer ions only to simplify the following discussion.

Figures 4a-4g show the TOF profiles of the NH_3^+ ions at the different degree of deceleration. With decreasing the voltage of the potential switch from 0 to -0.2 V, the mean velocity of the ions slows down to less than 177 m/s (Fig. 4g), which correspond to the kinetic energy of 2.8 meV. Figure 4g also exhibits a cut off of the TOF profile at the time of longer than about 17 ms, which corresponds to the velocity of 134 m/s (1.5 meV). This result indicates that the NH_3^+ ions with the kinetic energy of less than 1.5 meV do not reach to the detector due to a stray field still remains in the NMR cell. And also, the bunching of the ions becomes not efficient with the decreasing the mean velocity.

3.2 Cooling ion packet by velocity selection

In order to cool the ions further in the NMR cell, the velocity selection is carried out using the mesh electrodes mounted at the upstream of the front gate as shown in (a) of Fig. 2. The pair of mesh electrodes works as the velocity selector; a portion of the ions in the velocity distribution is sliced out and is restored in the cell as follow. When the ion packet comes up to the front gate after travelling N round-trips in the cell, the trap voltage is reduced to 0 V and, and at the same time, a positive pulse with a suitable duration is applied to the mesh installed at a upstream side. With these procedures, only the center portion of the ion packet is restored in the NMR cell and the rest of the ions escapes from the confinement. As an example, the time profiles up to $N = 5$ for the ion packet injected with $v_0 = 274$ m/s are shown in Fig. 5a, while, those sliced at $N = 2$ are shown in Fig. 5b. The pulse width and the amplitude applied to the mesh electrode are set at 200 μs and 0.5 V, respectively. As seen in Fig. 5a, the width of the ion packet becomes broad with increasing the number of round trips. These changes are a thermal broadening due to the initial velocity distribution width (Δv_0). As discussed in the previous paper [7], Δv_0 is obtained from the time profiles by the $\Delta t - t_C$ plot, where t_C and Δt are the center and the width of each time-profile peak, computed by fitting the observed peaks with assuming a Gaussian function. Without the slicing, the slope of the plot gives the velocity distribution width as $\Delta v_0 = 20$ m/s. After the slicing, Δv is calculated to be 2.4 m/s FWHM. Thus, the velocity distribution width is reduced by about one tenth with the velocity selection using the slicing technique. By assuming the velocity distribution of the ions as a one-dimensional Maxwell-Boltzmann type, Δv can be related to the translational temperature [7]. The width before the slicing (20 m/s) corresponds to

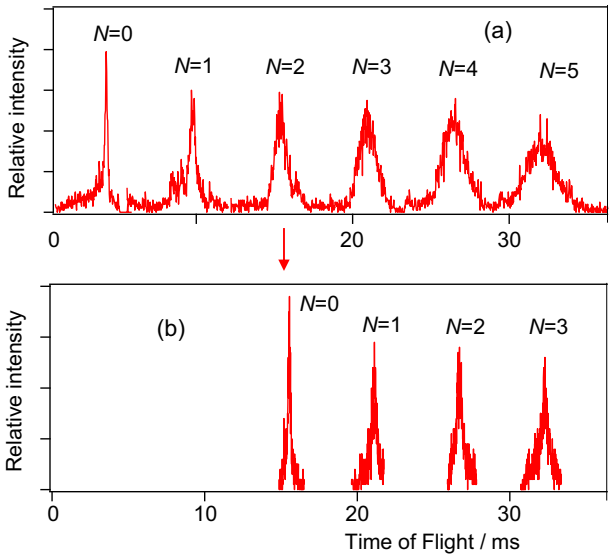

Fig. 5 Time-of-flight profiles of NH_3^+ ion packet (**a**) after injecting the NMR cell and (**b**) after slicing at the second round-trips (N =2) are shown. The pulse duration for slicing is 200 μs. The peaks for $N = 0 - 3$ in Fig. 5b are those traveling in the NMR cell after the slicing for (N+2)th round trips

the translational temperature as 0.16 K, and after the velocity selection, the temperature successfully reaches down to 2.2 mK. As described in Section 2.1, however, the velocity distribution width must be less than 1 m/s FWHM to facilitate the NMR detection for NH_3^+. Thus we still need to improve the cooling technique for molecular ions.

During the course of these studies, we found a very effective velocity selection procedure for p-xylene ions as a sample. In this experiment, a negative offset voltage of a few 100 mV was applied to the front gate in advance at the time of the velocity selection. A preliminary result indicates that the velocity distribution width was reduced further down to about 0.4 m/s FWHM (0.3 mK) . In order to clarify the mechanism to generate the extremely narrow velocity distribution width, we carried out a simulation on the velocity selection process using a software, Simion. The calculated results indicate that the negative offset voltage on the front gate induces a dispersion compensation of the distribution of the velocity-selected ions, which is similar to the bunching process. In order to succeed in detecting the first NMR signals of the gas-phase molecular ions, we are currently conducting the experiments including the improvement of the cooling technique based on these results.

4 Summary

NMR technique is a powerful tool to study the physical and chemical properties of materials in wide area. However, this technique is limited to the materials in condensed phase because of its very low sensitivity. In order to break this situation and to overcome the sensitivity problem, we proposed the new principle to detect the NMR of gas-phase molecular ions based on the Stern-Gerlach type experiment in the Penning trap. In this method, the ultra-cold molecular ions are introduced in the trap and their magnetic moments are probed by observing the modulation of their TOFs induced by the RF magnetic excitation at both ends

of the trap. To realize the NMR detection, we constructed the gas-phase NMR apparatus for mass selected ions. We are developing the methods to prepare and manipulate cold molecular ions under the strong magnetic field. Here, we discussed the experimental techniques and the results on the formation and manipulation of cold NH_3^+ ions with the kinetic energy of less than 3 meV, which are prepared through deceleration, bunching and slicing of the ion packets generated by the photoionization of supersonically cooled ammonia molecules. We also discussed the subjects on the NMR detection for cold mass-selected ions. These results on the basic performance of the present apparatus suggest that the first NMR signal for polyatomic ions will be detected in near future.

Acknowledgments This work has been supported by the research grant from the Japan Science and Technology Agency and by the Grant-in-Aid for Scientific Research (Grants # 24350009) from the Ministry of Education, Culture, Sports, Science, and Technology (MEXT) of Japan. We thank the Equipment Development Center of IMS for technical supports.

Compliance with Ethical Standards We warrant that the manuscript is an original work and has not been published before. We confirm that the manuscript meets the highest ethical standards.

References

1. Fukushima, E., Roeder, S.B.: Experimental Pulse NMR. Westview Press (1993)
2. Sinz, A.: Mass Spectrom. Rev. **25**, 663 (2006)
3. Syrstad, E.A., Turecek, F.: J. Am. Soc. Mass Spectrom. **16**, 208 (2005)
4. Rabi, I.I., Millman, S., Kusch, P., Zacharias, J.R.: Phys. Rev. **55**, 526 (1939)
5. Ulmer, S., Rodegheri, C.C., Blaum, K., Kracke, H., Mooser, A., Qunt, W., Walz, J.: Phys. Rev. Lett. **106**, 253001-1 (2011)
6. Van Dyck, R.S., Schwinberg, P.B., Dehmelt, H.: Phys. Rev. Lett. **59**, 26 (1987)
7. Fuke, K., Tona, M., Fujihara, Ishikawa, H.: Rev. Sci. Instrum. **83**, 085106-1-8 (2012)
8. Kominato, K., Takeda, M., Minami, I., Hirose, R., Ozaki, O., Ohta, H., Tou, H., Ishikawa, H., Sakurai, M., Fuke, K.: IEEE Trans. Appl. Supercond. **20**, 736 (2010)
9. Schnell, M., Meijer, G.: Angew. Chem. Int. Ed. **48**, 6010 (2009)
10. Gerlich, D.: The production and study of ultra-cold molecular ions. In: Smith, I.W.M. (ed.) Low temperatures and cold molecules, pp. 295–343. Imperial College Press (2008)
11. Larson, D.J., Bergquist, J.J., Itano, W.M., Wineland, D.J.: Phys. Rev. Lett. **57**, 70 (1986)
12. Ostendorf, A., Zhang, C.B., Wilson, M.A., Offenberg, D., Roth, B., Schiller, S.: Phys. Rev. Lett. **97**, 243005 (2006)
13. Anderson, J.B., Fenn, J.B.: Phys. Flu. **8**, 780 (1965)